doi:10.1016/j.jmb.2007.01.024 *J. Mol. Biol.* (2007) **367**, 925–934

JMB

Available online at www.sciencedirect.com

ScienceDirect

ELSEVIER

COMMUNICATION

Crystal Structure of the Streptococcal Superantigen SpeI and Functional Role of a Novel Loop Domain in T Cell Activation by Group V Superantigens

Jean-Nicholas P. Brouillard[1,2]†, Sebastian Günther[3]†, Ashok K. Varma[3] Irene Gryski[1,2], Christine A. Herfst[1,2], A. K. M. Nur-ur Rahman[1,2] Donald Y. M. Leung[4], Patrick M. Schlievert[5], Joaquín Madrenas[1,6] Eric J. Sundberg[3]* and John K. McCormick[1,2]*

[1]*Department of Microbiology and Immunology, The University of Western Ontario London, ON, Canada N6A 5B8*

[2]*Lawson Health Research Institute, London ON, Canada N6A 4V2*

[3]*Boston Biomedical Research Institute, Watertown MA 02472, USA*

[4]*Department of Pediatrics Dermatology and Medicine University of Colorado Health Sciences Center and Division of Pediatric Allergy and Immunology, The National Jewish Medical and Research Center, Denver, CO 80206, USA*

[5]*Department of Microbiology University of Minnesota Medical School, Minneapolis, MN 55455 USA*

[6]*The FOCIS Centre for Clinical Immunology and Immunotherapeutics, and Robarts Research Institute London, ON, Canada N6A 5K8*

**Corresponding authors*

Superantigens (SAgs) are potent microbial toxins that bind simultaneously to T cell receptors (TCRs) and class II major histocompatibility complex molecules, resulting in the activation and expansion of large T cell subsets and the onset of numerous human diseases. Within the bacterial SAg family, streptococcal pyrogenic exotoxin I (SpeI) has been classified as belonging to the group V SAg subclass, which are characterized by a unique, relatively conserved ~15 amino acid extension (amino acid residues 154 to 170 in SpeI; herein referred to as the α3–β8 loop), absent in SAg groups I through IV. Here, we report the crystal structure of SpeI at 1.56 Å resolution. Although the α3–β8 loop in SpeI is several residues shorter than that of another group V SAg, staphylococcal enterotoxin serotype I, the C-terminal portions of these loops, which are located adjacent to the putative TCR binding site, are structurally similar. Mutagenesis and subsequent functional analysis of SpeI indicates that TCR β-chains are likely engaged in a similar general orientation as other characterized SAgs. We show, however, that the α3–β8 loop length, and the presence of key glycine residues, are necessary for optimal activation of T cells. Based on Vβ-skewing analysis of human T cells activated with SpeI and structural models, we propose that the α3–β8 loop is positioned to form productive intermolecular contacts with the TCR β-chain, likely in framework region 3, and that these contacts are required for optimal TCR recognition by SpeI, and likely all other group V SAgs.

© 2007 Elsevier Ltd. All rights reserved.

Keywords: superantigens; *Streptococcus pyogenes*; T cell receptor

† J.-N. P. B. and S. G. contributed equally to this work.

Present addresses: J.-N. P. Brouillard, Department of Microbiology and Infectious Diseases, University of Calgary, Calgary AB, Canada T2N 4N1; S. Günther, Max-Delbrück-Center for Molecular Medicine, Robert-Rössle-Str. 10, 13125 Berlin, Germany.

Abbreviations used: SAg, superantigen; TCR, T cell receptor; SpeI, streptococcal pyrogenic exotoxin I; MHC, major histocompatibility complex; Vβ, variable region of the T cell receptor β-chain; CDR, complementarity determining region; TSS, toxic shock syndrome; TSST-1, toxic shock syndrome toxin-1; Spe, streptococcal pyrogenic exotoxin; HV, hypervariable; FR, framework region; TEV, tobacco etch virus; PBMCs, peripheral blood mononuclear cells.

E-mail addresses of the corresponding authors: sundberg@bbri.org; john.mccormick@schulich.uwo.ca

0022-2836/$ - see front matter © 2007 Elsevier Ltd. All rights reserved.

Superantigens (SAgs) are immunostimulatory molecules of microbial origin that function to activate large numbers of T cells by binding simultaneously to both major histocompatibility (MHC) class II molecules and T cell receptors (TCRs). SAg binding to MHC class II occurs outside of the peptide-binding groove, and can occur through two independent sites.[1,2] Binding to the TCR occurs through the variable region of the TCR β-chain (termed Vβ), and together with the MHC class II interactions, this prevents the complementarity determining region (CDR) loops from recognizing the antigenic peptide bound in the MHC class II molecule.[3] Thus, the hallmark of superantigenicity is a primary immune response that results in the activation of T cell subsets that are not specific for the antigenic peptide contained within the MHC class II cleft, but is dependent on which Vβ is engaged by the particular SAg.[4] In humans, the number of different TCR Vβs is limited to 56, comprising 26 major classes of β-chains in the TCR repertoire.[5,6] Because SAgs may bind to more than one Vβ, these potent toxins are thus capable of activating a large proportion of T cells, and their hyperactivation, and the subsequent release of large quantities of cytokines, is believed to result in various immune-mediated diseases including toxic shock syndrome (TSS).[7]

Evolutionary classification of the pyrogenic toxin bacterial SAgs

SAgs belonging to the pyrogenic toxin class include toxic shock syndrome toxin-1 (TSST-1) and the staphylococcal enterotoxins from *Staphylococcus aureus*, as well as the streptococcal pyrogenic exotoxins (Spes) from β-hemolytic streptococci, primarily *Streptococcus pyogenes*. Bacterial genome sequencing projects have revealed that a large number of genetically distinct SAgs are present in these bacterial pathogens, with more than 30 distinct SAg serotypes.[8] Sequence identities between the various SAgs can range from below 5% for distantly related members, to >95% for closely related SAgs. Although there are only a limited number of invariant residues among the pyrogenic toxin SAgs,[9] each are believed to share a conserved tertiary structure, and five distinct evolutionary groups have been proposed for these toxins (Figure 1).[7] Within this classification, TSST-1 from *S. aureus* is the only group I SAg, and this toxin is believed to be responsible for essentially all cases of menstruation-associated TSS.[12,13] TSST-1 is unique in that it binds MHC class II through an N-terminal, low-affinity binding domain that is peptide-dependent,[14,15] and engages the TCR Vβ through two independent regions within both CDR2 and framework region (FR) 3.[16,17] Group II SAgs contain both staphylococcal and streptococcal SAgs that also bind the MHC class II α-chain through an N-terminal, low-affinity binding domain; however, in contrast to group I, this binding is peptide-independent.[18] Group II SAgs include SEB, SEC and SpeA, which engage TCR Vβ through mostly conformation-dependent mechanisms that are largely independent of specific Vβ amino acid side-chains.[19–21] After TSST-1, SEB is believed to be most commonly linked with non-menstrual-associated cases of staphylococcal TSS,[22] while SpeA is most commonly linked with streptococcal TSS.[23] Group III SAgs consist of only staphylococcal SAgs, and these toxins are able to cross-link MHC class II molecules[1,2] through a low-affinity site similar to Group II,[24] as well as a high-affinity, zinc-dependent MHC class II binding interface located within the β-grasp domain of the SAg.[25] In general, group III SAgs (such as SEA) are most commonly associated with staphylococcal food-borne illness.[26] There is currently little available information regarding how group III SAgs engage TCR Vβ. Group IV SAgs are restricted to only streptococcal members, and these toxins contain a high-affinity MHC class II binding domain similar to group III.[27] Some members of this group (such as SpeC) have been proposed to lack the low-affinity MHC binding domain,[28] yet this remains controversial.[29,30] The structure of SpeC in complex with

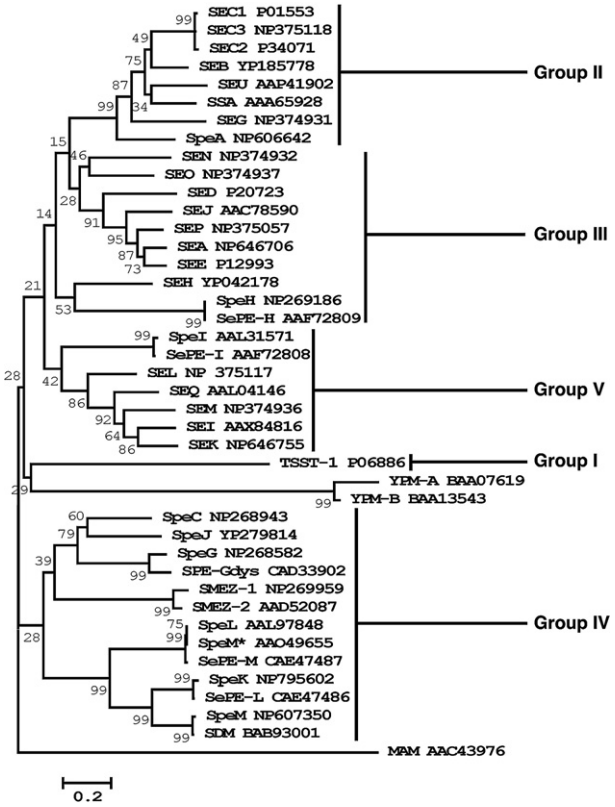

Figure 1. Neighbour–joining tree showing phylogenetic relationships of known bacterial superantigens. The unrooted tree was based on the alignment of amino acid sequences using CLUSTAL W[10] and constructed using MEGA3.1.[11] The SAg abbreviations are indicated followed by the relevant accession number. As previously proposed,[7] the five main groups of SAgs belonging to the pyrogenic toxin class are indicated, and the MAM and YPM SAgs are also included in the analysis. Numbers on branches are percentages from 1000 bootstraps, supporting a given partitioning.

human Vβ2.1 revealed the distinctive nature by how group IV SAgs engage Vβ. SpeC made multiple contacts with both side-chain and main-chain atoms of Vβ2.1, and was unique among characterized SAg–TCR interactions in that all three CDR loops were engaged, as well as hypervariable (HV) region 4 and FR3.[21] Also, the buried surface of the SpeC-Vβ2.1 interface was comparable to that of TCR–peptide–MHC complexes, considerably larger than the contact surfaces for other SAg–TCR complexes.[19–21] Recently, we have shown that a hotspot binding pocket on the surface of SpeC which is critical for activity, targets a non-canonical amino acid insertion found in the CDR2 loop of Vβ2, revealing how SpeC is highly selective for certain TCR Vβs.[31] Based on these collective characteristics, it is clear that the SAg evolutionary groups I through IV each display key differences in how they engage their host receptors.

Group V SAgs include the streptococcal SAg SpeI, and staphylococcal enterotoxin serotypes I, K, L, M and Q. The β-grasp motif of the C-terminal domain of SEI has been recently shown crystallographically to interact with the β1 domain α-helix of HLA–DR1 and the N-terminal portion of the bound antigenic peptide.[32] This interaction is highly similar to the interaction between SpeC with HLA–DR2a,[27] and SEH with HLA–DR1.[25] A unique feature of group V SAgs, however, is the presence of a loop extension between the third α-helix and the eighth β-sheet (which we term the α3–β8 loop) (Figure 2(a)). This homologous ~15 amino acid residue extension is not found in the other SAg groups,[7] and although SEI has been shown to bind human TCR Vβs 1 and 5.2,[39] the functional relevance of this loop has yet to be examined.

Expression, purification and crystallization of SpeI

Wild-type SpeI was PCR amplified from *S. pyogenes* SF370 chromosomal DNA and cloned into the pET28a expression vector (Novagen) using *Escherichia coli* XL1-blue as the cloning host (Stratagene). The forward primer amplified *speI* lacking the region encoding the predicted signal peptide and additionally, engineered a tobacco etch virus (TEV) protease cleavage site (ENLYFQG) which replaced the pET28a enterokinase cleavage site (DDDDK) upstream of the *speI* gene. The resulting plasmid (pET28a::TEV::SpeI) created an N-terminal translational fusion of the His_6 purification tag with SpeI, as well as the TEV site for removal of the purification tag. SpeI was expressed from *E. coli* BL21 (DE3) (Novagen) essentially as described[40] and purified on a nickel affinity column (Novagen). Recombinant, autoinactivation-resistant His_7::TEV was produced as described[41] and SpeI was cleaved overnight at 4 °C. The cleaved purification tag and His_7::TEV were subsequently removed by passage over the nickel column in binding buffer containing 15 mM imidazole. Purification was evaluated by SDS–PAGE and recombinant SpeI ran as a homogeneous, distinct ~27 kDa band. Protein concentrations were determined using a modified Bradford assay (Bio-Rad).

Wild-type SpeI, which contains a single cysteine residue at position 80, crystallized as inseparable bundles of small rods and SDS–PAGE analysis revealed that it existed in a monomer–dimer equilibrium. Addition of reducing agent to the crystallization stock solution and/or well solutions only marginally improved crystal morphology. Thus, the Cys80 residue in SpeI was mutated to a serine by site-directed mutagenesis. The SpeI C80S mutant crystallized as thin plates in 30% (w/v) PEG 4000, 0.2 $MgCl_2$, 0.1 M Tris–HCl (pH 8.5) and crystals were significantly improved using micro-seeding techniques to produce single crystals measuring ~0.3 mm × 0.5 mm × 0.1 mm. A complete data set to a nominal resolution of 1.9 Å was collected at CHESS, beam line A-1, and processed using HKL2000.[33] Surprisingly, no molecular replacement solution could be determined using any of numerous homologous SAg structures and molecular replacement programs. Thus, a strategy for determining the structure by multi-wavelength anomalous dispersion (MAD) phasing was pursued. Because SpeI contains only two methionine residues, one of which is very near the N terminus and was likely to be disordered in the crystal, three additional methionine residues were engineered into the SpeI C80S mutant. The resulting SpeI C80S/L14M/L55M/L190M mutant was produced as a seleno-methionine derivative in the *E. coli* auxotrophic strain B384. The presence of five seleno-methionine residues in the purified protein was verified by mass spectrometry. SpeI C80S/L14M/L55M/L190M was crystallized according to the micro-seeding method used to crystallize SpeI C80S.

Overview of the SpeI structure

The structure of the group V SAg SpeI was determined by X-ray crystallography to a resolution of 1.56 Å (Table 1). The SpeI structure is highly similar to that of the group V SAg SEI,[32] and conforms to the classical bacterial SAg fold that is comprised of N-terminal β-barrel and C-terminal β-grasp domains connect by a central α-helix (Figure 2(a)). All residues in the structure exhibited unambiguous electron density, including the α3–β8 loop (discussed below).

SpeI has been shown to bind MHC class II molecules in a zinc-dependent manner.[42] SpeI and SEI show 39% identity, and the juxtaposition of residues His179, His217 and Asp219 in the SpeI crystal structure (Figure 2(b)) is nearly identical to that of SEI[32] and other SAgs that bind to the β subunit of MHC class II molecules.[25,27] A 4.0σ peak was observed at a position that satisfies zinc coordination between these three residues in the final electron density map of the SpeI structure. This indicates that SpeI likely engages MHC class II molecules in a nearly identical way to that of SEI.

The primary amino acid sequence comparison of various pyrogenic toxin SAgs from each group clearly shows the extended loop characteristic of the

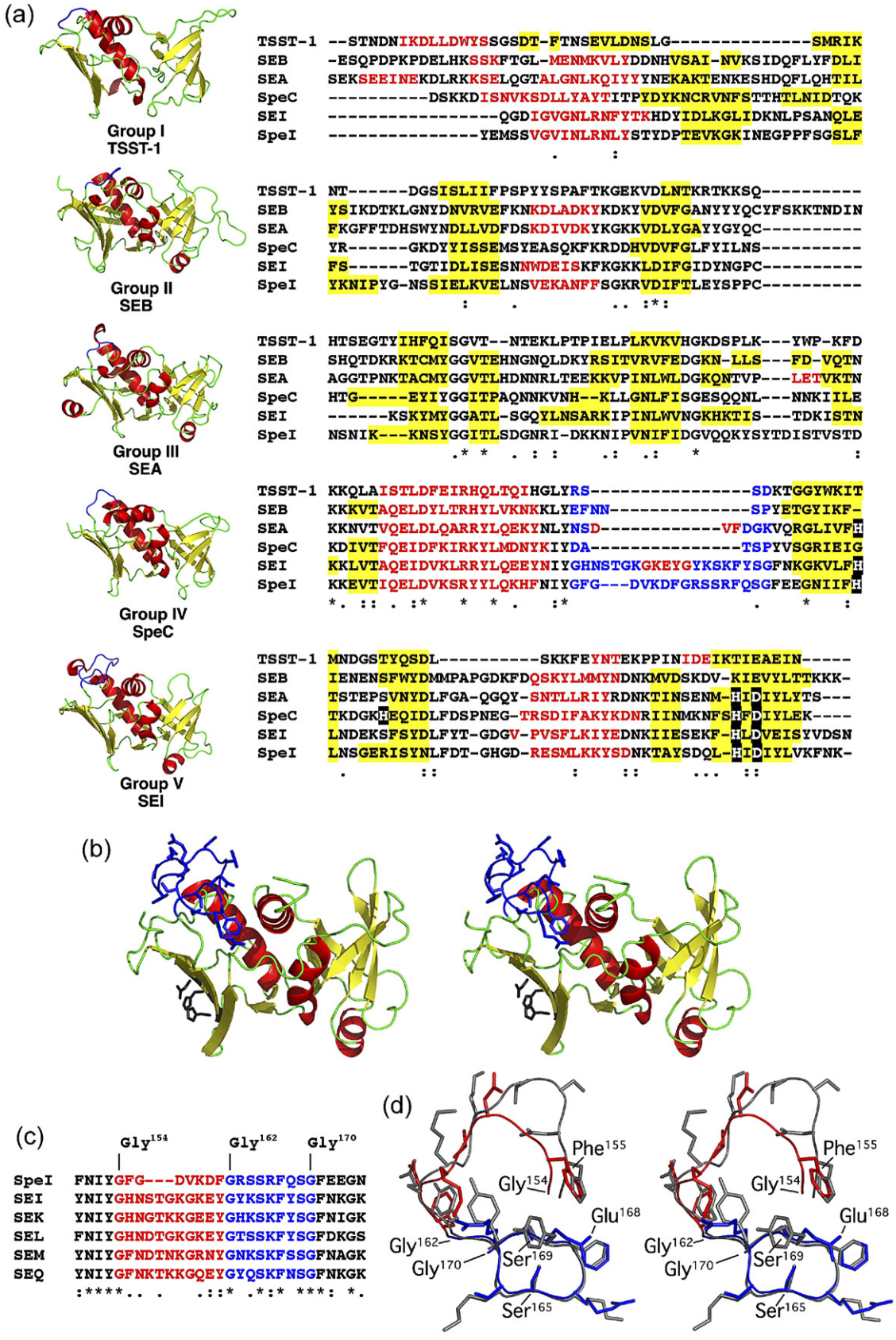

Figure 2 (*legend on opposite page*)

Table 1. Crystallographic data collection, processing and refinement statistics

A. *Data collection and processing*				
Space group	$P2_1$			
Unit cell dimensions	$a=30.9$ Å, $b=80.5$ Å, $c=43.1$ Å, $\beta=99.5°$			
	Peak	Edge	Remote	
Wavelength (Å)	0.979029	0.979416	0.964183	
Resolution (Å)	50–1.56	50–1.56	50–1.54	
Mosaicity (°)	0.5	0.5	0.5	
Observations	202,346	203,810	213,465	
Unique reflections	57,515	57,543	59,966	
Completeness (%)	98.8 (91.3)[a]	98.8 (91.2)	99.3 (95.7)	
Mean I/σ (I)	28.6 (7.7)	28.3 (7.6)	28.2 (6.8)	
R_{sym} (%)[b]	4.1 (12.9)	4.5 (13.1)	4.5 (14.4)	
B. *MAD phasing statistics*				
Se atoms found	4			
Figure of merit	0.71			
C. *Refinement*				
R_{work} (%)[c]	17.6			
R_{free} (%)[d]	22.7			
Protein residues	227			
Water molecules	299			
Average B factor (Å^2)	15.2 (Protein residues)		28.4 (Water molecules)	
RMS deviations	0.01 (Bonds, Å)	1.3 (Angles, °)		
Ramachandran plot statistics[e]	89.5 (Core, %)	8.5 (Allowed, %)	0.5 (Generous, %)	1.5 (Disallowed, %)

[a] Values in parentheses correspond to the highest resolution shell (Peak, Edge, Remote: 1.60 Å–1.54 Å).
[b] $R_{sym}=\sum|((I_{hkl}-I_{(hkl)})|/(\sum I_{hkl})$, where $I_{(hkl)}$ is the mean intensity of all reflections equivalent to hkl by symmetry.
[c] $R_{work}=\sum||F_O|-|F_C|/\sum|F_O||$, where F_C is the calculated structure factor.
[d] R_{free} is calculated over reflections in a test set not included in atomic refinement: 1489 reflections, 5.1%.
[e] Residues in disallowed regions include Ser34, Ser47 and Ser80. Each of these residues is part of β-turn element. The first two of these residues are modelled into unambiguous electron density, while the third is modelled into relatively ambiguous electron density.

group V SAgs,[7] relative to the other four classes (Figure 2(a)). The most similar region occurs in group III SAgs, yet this loop is still nine amino acids shorter (in SEA) compared with SpeI (Figure 2(a)). In SpeI and SEI, this loop follows the central α-helix that connects the two conserved domains. Of all the group V SAgs, the SpeI α3–β8 loop is the least homologous, as each of the staphylococcal enterotoxin loops are extended by an additional 3 residues (Figure 2(c)). These three residues (Ser144, Tyr145 and Gly146 in SEI) reside in the N-terminal portion of the loop and result in a more extended turn in this region for SEI relative to SpeI and thus the majority of variation in both sequence and structure is seen between residues Gly154 and Gly162 (relative to the SpeI sequence) (Figure 2(c) and (d)). Natural variants within the α3–β8 loop of SEI that differed at positions Asn143 and Ser144 did not apparently alter the T cell stimulatory capacity of these variants.[39] The C-terminal portion of the α3–β8 loop, however, is essentially identical in structure between these two SAgs such that after residue Phe161 of SpeI (Tyr151 in SEI) the loops are virtually superimposable (Figure 2(d)).

Figure 2. Crystal structure of SpeI and comparison with SAg representatives for each SAg group. (a) Representative ribbon diagram crystal structures and amino acid sequence alignments for group I (TSST-1), group II (SEB), group III (SEA), group IV (SpeC), and group V (SEI) SAgs. Colouring is according to the secondary structure where α-helices are coloured red and β-sheets are coloured yellow, and the three residues involved in coordinating zinc for binding to the β1 domain of MHC class II are boxed in black. The α3–β8 loop in group V SAgs, and similar regions in groups I–IV are shown in blue. (b) Stereo view ribbon diagram of the molecular structure of SpeI. The structure of SpeI was determined by MAD phasing. Complete diffraction data to 1.56 Å resolution at three distinct wavelengths (at the selenium peak, edge and remote wavelengths) was collected at CHESS, beam line F-1 and processed using HKL2000.[33] The positions of four of the five heavy atoms were determined using SOLVE[34] and a partial model was built automatically using RESOLVE.[34,35] The structure was refined using CNS[36] interspersed with manual model building in Coot.[37] Colouring is according to the secondary structure as in (a) and side-chains of the α3–β8 loop (blue) and zinc coordinating residues (black) are shown as stick representations. (c) Alignment of the α3–β8 loop from group V SAgs. The SePE-I α3–β8 loop from *Streptococcus equi* (not shown)[38] is identical to that of SpeI. The highly conserved region is shown in blue, and the remainder of the loop is shown in red. Numbering of the glycine residues is according to the SpeI sequence. (d) Stereo view comparison of the structurally aligned α3–β8 loops from SEI[32] (black) and SpeI (residues Gly154 to Phe161 are shown in red and residues Gly162 to Gly170 are shown in blue). The conserved SpeI residues Gly154, Gly162, Ser165, Ser169 and Gly170 are indicated, as well as Phe155 and Glu168 that are proposed to interact with FR3. Structural representations were generated using MacPyMOL [http://pymol.sourceforge.net/].

Alanine-scanning mutagenesis of the predicted TCR Vβ binding site on SpeI

Bacterial SAgs appear to universally bind the CDR2 loop, but there are at least three distinct modes for how SAgs engage the TCR Vβ represented by SEB, SEC and SpeA for group II SAgs, SpeC for group IV SAgs, and TSST-1 as the only group I SAg. SpeC binds in a slightly different orientation to the group II SAgs, with a larger buried surface area, and generally targets TCR Vβ side-chain atoms[21] while the SEB/SEC/SpeA binding mode generally targets TCR Vβ main-chain atoms.[19–21] The TSST-1 binding mode for TCR Vβ engages a distinct surface which overlaps with the first two, but also makes important contacts through residues within the SAg central α-helix that engage FR3.[16,17,43] To first evaluate if SpeI engages TCR Vβ in a similar orientation to other SAgs, candidate residues Asn13, Tyr44, Ser77, Lys86 and Arg198 were each individually targeted for alanine-scanning mutagenesis.[44] These residues were based on locations known to interact with TCR Vβ chains similar to SEB,[20] SEC,[19] SpeA[21] or SpeC,[21] and each line a pocket in SpeI that could potentially bind regions of the TCR Vβ, most likely the CDR2 loop. Furthermore, based on the atypical positioning of the Vβ binding region of TSST-1,[16,17,43] Tyr144 (equivalent position to His135 in TSST-1 which is critical for engagement of TCR Vβ) was also targeted for mutation. The various single-site SpeI mutants were tested to induce dose-dependent proliferation of human peripheral blood mononuclear cells. Mutants N13A, S77A, and R198A each displayed a 5 to 25-fold reduction in potency, compared with wild-type SpeI (Figure 3(a)), whereas mutants Y44A, K86A and Y144A exhibited no apparent relative change in activity. These data are consistent with other known SAg–TCR inter-

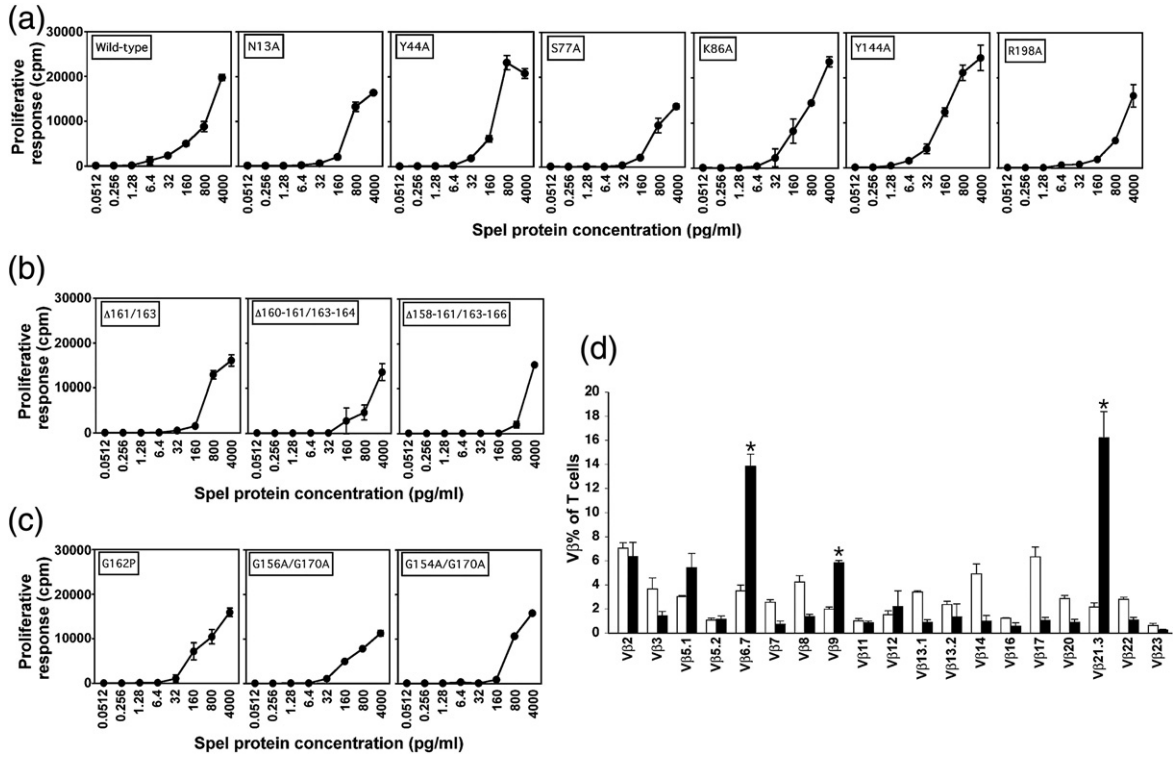

Figure 3. Dose-dependent T-cell proliferation curves for the various site-specific and deletion mutations of SpeI. The SpeI mutants were generated using an overlapping megaprimer PCR method with oligonucleotides that incorporated the desired mutation and individual proteins were produced as described for wild-type SpeI. Representative proliferation curves for (a) alanine-scanning mutations within the predicted TCR Vβ binding site on SpeI; (b) deletion mutations within the α3–β8 loop; and (c) mutations that targeted conserved glycine residues within the α3–β8 loop. Proliferation was assessed by the incorporation of [^{3}H]thymidine into human peripheral blood mononuclear cells (2×10^5/well) in response to incubation with serial fivefold dilutions of the various SpeI proteins. Cells were incubated in RPMI medium (Gibco) supplemented with 10% (v/v) fetal calf serum (Sigma), 100 μg/ml streptomycin (Sigma), 100 units/ml penicillin (Sigma), and 1% (w/v) L-glutamine (Sigma) in 5% (v/v) CO_2 at 37 °C with the various SpeI proteins for three days and then labelled with 1 μCi of [^{3}H]thymidine, and DNA was harvested after 18 h of incubation. The counts per minute were determined by scintillation counting and plotted at each concentration of protein. The bars represent the mean±the standard error for experiments done in triplicate. (d) Vβ skewing analysis of SpeI. Separate preparations of peripheral blood mononuclear cells were obtained from four normal human donors and 10^6 cells/ml were cultured in the presence of either anti-CD3 antibody (20 ng/ml) or SpeI (100 ng/ml) for three days, washed, and allowed to grow for an additional day in the presence of interleukin-2 (50 units/ml) before washing and staining for immunofluoresence analysis of the Vβ T-cell repertoire as described.[45] Bars represent the percentage of total CD3$^+$ cells stimulated with SpeI (filled bars) or anti-CD3 (open bars), expressed as the mean±the standard error (*, $p<0.05$ when stimulation by SpeI was compared to stimulation by anti-CD3 antibodies as determined by the paired Student's t test).

actions,[16,17,19–21,31,43,46,47] and most likely indicate that the CDR2 loop of TCR Vβ is engaged within a cleft formed between the two domains of SpeI. None of the mutations resulted in a complete loss of activity. This suggests a loss of binding to one or more members of the wild-type Vβ-binding repertoire due to a lack of stabilizing interactions, but not to all Vβ targets simultaneously. The wild-type activity for the Y144A mutation indicates that SpeI does not likely engage TCR Vβ in a similar manner to TSST-1.

Reducing the SpeI α3–β8 loop length diminishes T cell activation

Based on the alanine-scanning mutagenesis data, it was apparent that the α3–β8 loop may be positioned to make contacts with the TCR Vβ, most likely within FR3. To address this possibility, we generated a series of three deletion mutants to shorten the overall length of the loop, where paired residues on either side of Gly162 were removed in an attempt to retain the overall loop organization. The mutants lacked a total of two, four and eight residues (SpeI mutants Δ161/163, Δ160-161/163-164, Δ158-161/163-166, respectively). The deletion mutants each showed a decrease in activity where the shorter the loop, the lower the potency of the SpeI mutant, up to a 125-fold reduction in activity for the SpeI Δ158-161/163-166 mutant (Figure 3(b)). These data indicate that the SpeI α3–β8 loop length, or conformation, is important for the engagement and subsequent activation of T cells.

Mutations in conserved α3–β8 loop glycine residues affect SpeI function

Residues Gly154, Gly162, Ser165, Phe167, Ser169, and Gly170 (relative to the SpeI sequence) are strictly conserved in all of the group V SAgs (Figure 2(c)), and each of these residues adopts a nearly identical position in the SpeI and SEI α3-β8 loops (Figure 2(d)). In particular, both Ser165 and Ser169 form a series of hydrogen bonding networks within both the α3–β8 loop and the SAg core, likely stabilizing this region of the α3–β8 loop to the surface of the β-grasp domain. From the primary amino acid sequence analysis, we initially hypothesized that the conserved glycine residues may contribute to the conformational flexibility of the α3–β8 loop, and that this would potentially contribute to TCR binding. However, the α3–β8 loops in SpeI and SEI exhibited unambiguous electron density with *B*-factors similar to the overall structures. Thus, it appears that these glycine residues do not contribute to flexibility, but allow the α3–β8 loop to adopt a favourable conformation for Vβ engagement. To address this, we targeted the paired glycine residues at the termini of the loop for mutagenesis, as well as Gly162 located near the middle of the loop (Figure 2(c)). The alanine substitutions at the paired terminal glycine residues (G156A/G170A and G154A/G170A) and the Gly→Pro substitution at position 162 each displayed a fivefold reduction in potency (Figure 3(c)). Together, these data indicate that the conformation of the α3–β8 loop is dependent on the conserved glycine residues for optimal engagement of the TCR Vβ.

Vβ-specificity of SpeI

Flow cytometry methods were used to determine the Vβ profile of recombinant SpeI (Figure 3(d)). From this analysis, proliferating T cells expressing Vβs 6.7, 9 and 21.3, were significantly expanded. Vβ5.1 also appeared to be expanded, yet this was not statistically significant ($p = 0.128$). A primary sequence alignment for Vβs 6.7, 9 and 21.3 revealed little sequence homology in the CDR2 and HV4 loops, which together represent the most common regions for engagement with bacterial SAgs.[21] However, the analysis of the Vβ sequences did reveal conserved regions in both the CDR1 loop and FR3, which could represent potential binding sites for SpeI. Using the Vβ6.2 TCR structure,[48] which is the closest structurally characterized homologue to Vβ6.7 targeted by SpeI, conserved residues that were both surface exposed and potentially capable of making SAg contacts occurred in CDR1 (residues Gly28 and His29), and FR3 region (residues Pro61, Arg64, Phe65 and Ser66). TSST-1 interacts with a similar region of FR3,[16] in particular residues Glu61 and Lys62 in Vβ2.1, which contribute to complex formation as hot spots for TSST-1 binding.[17] These two residues are located adjacent to the Arg-Phe-Ser motif in FR3 common to Vβ's 6.7, 9, and 21.3, and may represent a binding location for the α3–β8 loop.

Modeling TCR Vβ engagement by SpeI

Structural information regarding Vβ engagement by SAgs is available for group I (TSST-1),[16] group II (SEB, SEC and SpeA),[19–21] and group IV (SpeC) SAgs.[21] The engagement of Vβ by group V SAgs is not likely similar to TSST-1, as the SpeI Y144A mutant specific for the TSST-1 binding mode exhibited wild-type activity (Figure 3(a)). Additionally from our phylogenetic analysis, SpeI (and the other group V SAgs) clusters closer to group II than to group IV SAgs (Figure 1). Thus, we superimposed the SpeI structure, and the Vβ6.2 structure,[48] onto the group II SpeA-mVβ8.2 complex[21] (Figure 4(a)). Based on this model, the N and C termini of the SpeI α3–β8 loop face the TCR–Vβ chain suggesting that residues Phe155 and Gln168 could potentially interact directly with the Vβ FR3 region (Figure 2(d) and Figure 4(b)). The model is also supported by the alanine-scanning mutagenesis data, where residues Asn13, Ser77 and Arg198 would surround the CDR2 loop. Although the glycine mutations imply that flexibility of this loop could be important for the interaction, the *B*-factor indicates that this loop is relatively rigid, and that changes in the α3–β8 loop that affect T cell activation are likely a result of permutations in a region of the

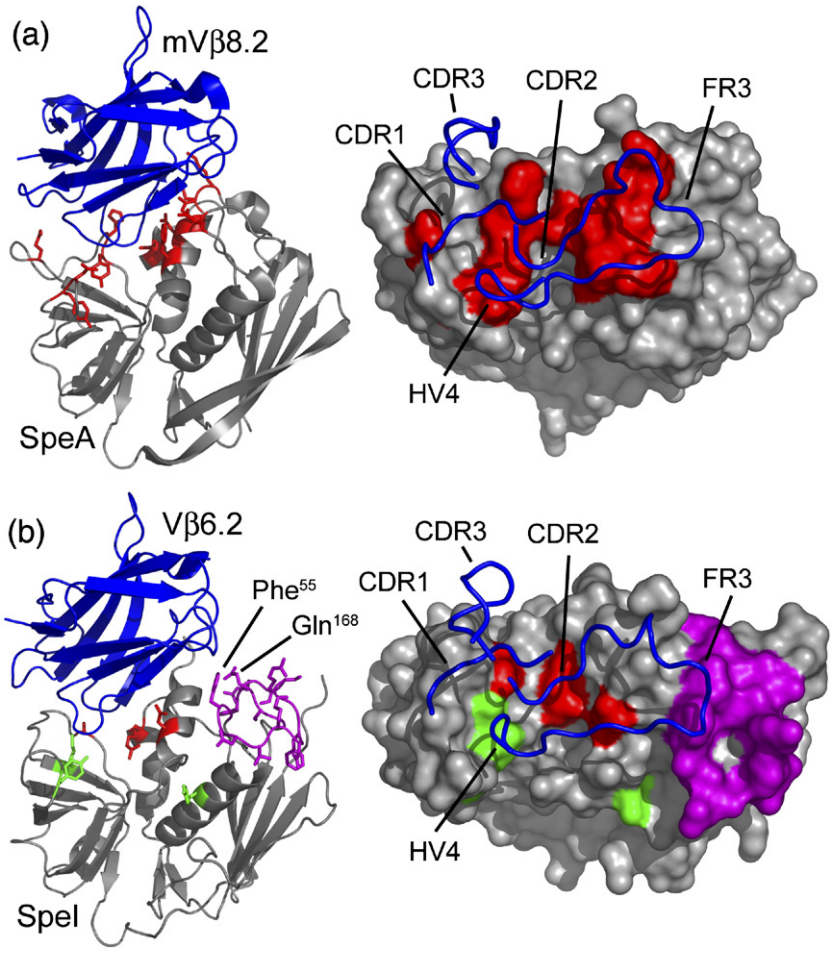

Figure 4. Modelled engagement of TCR Vβ by SpeI. (a) Ribbon diagram of the SpeA–mouse Vβ8.2 complex (PDB accession code 1L0Y).[21] The mouse Vβ8.2 chain is shown in blue (Cβ has been removed for clarity) and SpeA is shown in grey with amino acids that make intermolecular contacts with Vβ8.2 shown in red. The right panel shows the molecular surface of SpeA with amino acids that make specific contacts with Vβ8.2 in red. The CDR 1, 2 and 3 loops, as well as HV4 of Vβ8.2 are shown in blue with the remainder of the Vβ chain removed for clarity. (b) Modelled complex of the SpeI–Vβ6.2 by superimposition of the SpeI crystal structure (residues 4–227) presented here, and the crystal structure of human Vβ6.2 (PDB accession code 1MI5),[48] both superimposed onto the SpeA–mVβ8.2 complex shown in (a). SpeI residues Phe155 and Gln168, proposed to interact with FR3 are indicated. The right panel shows the molecular surface of SpeI with mutations having a negative functional impact as red, silent mutations as green, and residues Gly154 to Gly162 of the α3–β8 loop shown in magenta. The CDR and HV4 loops are shown as for (a).

loop with a common structural motif. The functional effects exhibited by SpeI variants that incorporate mutations in the α3–β8 loop are therefore anticipated to be broadly applicable to all group V SAgs.

In summary, we propose that the region between Gly154 and Gly162 of the α3–β8 loop is directly involved in TCR binding, the conserved glycine residues within this loop allow the loop to adopt a favourable binding conformation, and that the loop is necessary for the efficient activation of T cells. From this and other analyses, it appears that the different evolutionary SAg groups may each have evolved distinct architectures for engagement of their TCR ligands.

Protein Data Bank accession number

The atomic coordinates of the SpeI crystal structure have been deposited into the RCSB Protein Data Bank with the PDB accession number 2ICI.

Acknowledgements

We thank the staff at CHESS beam lines A-1 and F-1. This work was supported by Canadian Institutes of Health Research (CIHR) operating grants (to J. K. M. and J. M.), and National Institutes of Health grants AI55882 (to E. J. S.). J. M. holds a Canada Research Chair in Transplantation and Immunobiology, and J. K. M. holds a New Investigator award from the CIHR.

References

1. Hudson, K. R., Tiedemann, R. E., Urban, R. G., Lowe, S. C., Strominger, J. L. & Fraser, J. D. (1995). Staphylococcal enterotoxin A has two cooperative binding sites on major histocompatibility complex class II. *J. Exp. Med.* **182**, 711–720.
2. Abrahmsen, L., Dohlsten, M., Segren, S., Bjork, P., Jonsson, E. & Kalland, T. (1995). Characterization of two distinct MHC class II binding sites in the superantigen staphylococcal enterotoxin A. *EMBO J.* **14**, 2978–2986.
3. Li, H., Llera, A., Malchiodi, E. L. & Mariuzza, R. A. (1999). The structural basis of T cell activation by superantigens. *Annu. Rev. Immunol.* **17**, 435–466.
4. White, J., Herman, A., Pullen, A. M., Kubo, R., Kappler, J. W. & Marrack, P. (1989). The V beta-specific superantigen staphylococcal enterotoxin B: stimulation of mature T cells and clonal deletion in neonatal mice. *Cell*, **56**, 27–35.
5. Arden, B., Clark, S. P., Kabelitz, D. & Mak, T. W. (1995). Human T-cell receptor variable gene segment families. *Immunogenetics*, **42**, 455–500.
6. Wei, S., Charmley, P., Robinson, M. A. & Concannon, P. (1994). The extent of the human germline T-cell

receptor V beta gene segment repertoire. *Immunogenetics*, **40**, 27–36.
7. McCormick, J. K., Yarwood, J. M. & Schlievert, P. M. (2001). Toxic shock syndrome and bacterial superantigens: an update. *Annu. Rev. Microbiol.* **55**, 77–104.
8. Proft, T. & Fraser, J. D. (2003). Bacterial superantigens. *Clin. Exp. Immunol.* **133**, 299–306.
9. Arcus, V. L., Proft, T., Sigrell, J. A., Baker, H. M., Fraser, J. D. & Baker, E. N. (2000). Conservation and variation in superantigen structure and activity highlighted by the three-dimensional structures of two new superantigens from *Streptococcus pyogenes*. *J. Mol. Biol.* **299**, 157–168.
10. Thompson, J. D., Higgins, D. G. & Gibson, T. J. (1994). CLUSTAL W: improving the sensitivity of progressive multiple sequence alignment through sequence weighting, position-specific gap penalties and weight matrix choice. *Nucl. Acids Res.* **22**, 4673–4680.
11. Kumar, S., Tamura, K. & Nei, M. (2004). MEGA3: integrated software for molecular evolutionary genetics analysis and sequence alignment. *Brief Bioinform.* **5**, 150–163.
12. Bergdoll, M. S., Crass, B. A., Reiser, R. F., Robbins, R. N. & Davis, J. P. (1981). A new staphylococcal enterotoxin, enterotoxin F, associated with toxic-shock-syndrome *Staphylococcus aureus* isolates. *Lancet*, **1**, 1017–1021.
13. Schlievert, P. M., Shands, K. N., Dan, B. B., Schmid, G. P. & Nishimura, R. D. (1981). Identification and characterization of an exotoxin from *Staphylococcus aureus* associated with toxic-shock syndrome. *J. Infect. Dis.* **143**, 509–516.
14. Kim, J., Urban, R. G., Strominger, J. L. & Wiley, D. C. (1994). Toxic shock syndrome toxin-1 complexed with a class II major histocompatibility molecule HLA-DR1. *Science*, **266**, 1870–1874.
15. Wen, R., Cole, G. A., Surman, S., Blackman, M. A. & Woodland, D. L. (1996). Major histocompatibility complex class II-associated peptides control the presentation of bacterial superantigens to T cells. *J. Exp. Med.* **183**, 1083–1092.
16. Moza, B., Varma, A. K., Buonpane, R. A., Zhu, P., Herfst, C. A., Nicholson, M. J. *et al.* (2007). Structural basis of T cell specificity and activation by the bacterial superantigen toxic shock syndrome toxin-1. *EMBO J.* In the press.
17. Moza, B., Buonpane, R. A., Zhu, P., Herfst, C. A., Rahman, A. K., McCormick, J. K. *et al.* (2006). Long-range cooperative binding effects in a T cell receptor variable domain. *Proc. Natl Acad. Sci. USA*, **103**, 9867–9872.
18. Jardetzky, T. S., Brown, J. H., Gorga, J. C., Stern, L. J., Urban, R. G., Chi, Y. I. *et al.* (1994). Three-dimensional structure of a human class II histocompatibility molecule complexed with superantigen. *Nature*, **368**, 711–718.
19. Fields, B. A., Malchiodi, E. L., Li, H., Ysern, X., Stauffacher, C. V., Schlievert, P. M. *et al.* (1996). Crystal structure of a T-cell receptor beta-chain complexed with a superantigen. *Nature*, **384**, 188–192.
20. Li, H., Llera, A., Tsuchiya, D., Leder, L., Ysern, X., Schlievert, P. M. *et al.* (1998). Three-dimensional structure of the complex between a T cell receptor beta chain and the superantigen staphylococcal enterotoxin B. *Immunity*, **9**, 807–816.
21. Sundberg, E. J., Li, H., Llera, A. S., McCormick, J. K., Tormo, J., Schlievert, P. M. *et al.* (2002). Structures of two streptococcal superantigens bound to TCR beta chains reveal diversity in the architecture of T cell signaling complexes. *Structure (Camb.)*, **10**, 687–699.
22. Schlievert, P. M. (1986). Staphylococcal enterotoxin B and toxic-shock syndrome toxin-1 are significantly associated with non-menstrual TSS [letter]. *Lancet*, **1**, 1149–1150.
23. Stevens, D. L., Tanner, M. H., Winship, J., Swarts, R., Ries, K. M., Schlievert, P. M. & Kaplan, E. (1989). Severe group A streptococcal infections associated with a toxic shock- like syndrome and scarlet fever toxin A. *New Engl. J. Med.* **321**, 1–7.
24. Petersson, K., Thunnissen, M., Forsberg, G. & Walse, B. (2002). Crystal structure of a SEA variant in complex with MHC class II reveals the ability of SEA to crosslink MHC molecules. *Structure*, **10**, 1619–1626.
25. Petersson, K., Hakansson, M., Nilsson, H., Forsberg, G., Svensson, L. A., Liljas, A. & Walse, B. (2001). Crystal structure of a superantigen bound to MHC class II displays zinc and peptide dependence. *EMBO J.* **20**, 3306–3312.
26. Dinges, M. M., Orwin, P. M. & Schlievert, P. M. (2000). Exotoxins of *Staphylococcus aureus*. *Clin. Microbiol. Rev.* **13**, 16–34.
27. Li, Y., Li, H., Dimasi, N., McCormick, J. K., Martin, R., Schuck, P. *et al.* (2001). Crystal structure of a superantigen bound to the high-affinity, zinc-dependent site on MHC class II. *Immunity*, **14**, 93–104.
28. Li, P. L., Tiedemann, R. E., Moffat, S. L. & Fraser, J. D. (1997). The superantigen streptococcal pyrogenic exotoxin C (SPE-C) exhibits a novel mode of action. *J. Exp. Med.* **186**, 375–383.
29. Swietnicki, W., Barnie, A. M., Dyas, B. K. & Ulrich, R. G. (2003). Zinc binding and dimerization of *Streptococcus pyogenes* pyrogenic exotoxin C are not essential for T-cell stimulation. *J. Biol. Chem.* **278**, 9885–9895.
30. Tripp, T. J., McCormick, J. K., Webb, J. M. & Schlievert, P. M. (2003). The zinc-dependent major histocompatibility complex class II binding site of streptococcal pyrogenic exotoxin C is critical for maximal superantigen function and toxic activity. *Infect. Immun.* **71**, 1548–1550.
31. Rahman, A. K., Herfst, C. A., Moza, B., Shames, S. R., Chau, L. A., Bueno, C. *et al.* (2006). Molecular basis of TCR selectivity, cross-reactivity, and allelic discrimination by a bacterial superantigen: integrative functional and energetic mapping of the SpeC-Vbeta2.1 molecular interface. *J. Immunol.* **177**, 8595–8603.
32. Fernandez, M. M., Guan, R., Swaminathan, C. P., Malchiodi, E. L. & Mariuzza, R. A. (2006). Crystal structure of staphylococcal enterotoxin I (SEI) in complex with a human major histocompatibility complex class II molecule. *J. Biol. Chem.* **281**, 25356–25364.
33. Otwinowski, Z. & Minor, W. (1997). Processing X-ray diffraction data collected in oscillation mode. *Methods Enzymol.* **276**, 307–326.
34. Terwilliger, T. C. (2000). Maximum-likelihood density modification. *Acta Crystallog. sect. D*, **56**, 965–972.
35. Terwilliger, T. C. (2003). Automated main-chain model building by template matching and iterative fragment extension. *Acta Crystallog. sect. D*, **59**, 38–44.
36. Brunger, A. T., Adams, P. D., Clore, G. M., DeLano, W. L., Gros, P., Grosse-Kunstleve, R. W. *et al.* (1998). Crystallography and NMR system: a new software suite for macromolecular structure determination. *Acta Crystallog. sect. D*, **54**, 905–921.
37. Emsley, P. & Cowtan, K. (2004). Coot: model-building tools for molecular graphics. *Acta Crystallog. sect. D*, **60**, 2126–2132.
38. Artiushin, S. C., Timoney, J. F., Sheoran, A. S. & Muthupalani, S. K. (2002). Characterization and

immunogenicity of pyrogenic mitogens SePE-H and SePE-I of *Streptococcus* equi. *Microb. Pathog.* **32**, 71–85.
39. Fernandez, M. M., De Marzi, M. C., Berguer, P., Burzyn, D., Langley, R. J., Piazzon, I. *et al.* (2006). Binding of natural variants of staphylococcal superantigens SEG and SEI to TCR and MHC class II molecule. *Mol. Immunol.* **43**, 927–938.
40. McCormick, J. K. & Schlievert, P. M. (2003). Expression, purification, and detection of novel streptococcal superantigens. *Methods Mol. Biol.* **214**, 33–43.
41. Kapust, R. B., Tozser, J., Fox, J. D., Anderson, D. E., Cherry, S., Copeland, T. D. & Waugh, D. S. (2001). Tobacco etch virus protease: mechanism of autolysis and rational design of stable mutants with wild-type catalytic proficiency. *Protein Eng.* **14**, 993–1000.
42. Proft, T., Arcus, V. L., Handley, V., Baker, E. N. & Fraser, J. D. (2001). Immunological and biochemical characterization of streptococcal pyrogenic exotoxins I and J (SPE-I and SPE-J) from *Streptococcus pyogenes*. *J. Immunol.* **166**, 6711–6719.
43. McCormick, J. K., Tripp, T. J., Llera, A. S., Sundberg, E. J., Dinges, M. M., Mariuzza, R. A. & Schlievert, P. M. (2003). Functional analysis of the TCR binding domain of toxic shock syndrome toxin-1 predicts further diversity in MHC class II/superantigen/TCR ternary complexes. *J. Immunol.* **171**, 1385–1392.
44. Wells, J. A. (1991). Systematic mutational analyses of protein-protein interfaces. *Methods Enzymol.* **202**, 390–411.
45. McCormick, J. K., Pragman, A. A., Stolpa, J. C., Leung, D. Y. & Schlievert, P. M. (2001). Functional characterization of streptococcal pyrogenic exotoxin J, a novel superantigen. *Infect. Immun.* **69**, 1381–1388.
46. Hudson, K. R., Robinson, H. & Fraser, J. D. (1993). Two adjacent residues in staphylococcal enterotoxins A and E determine T cell receptor V beta specificity. *J. Exp. Med.* **177**, 175–184.
47. Churchill, H. R., Andersen, P. S., Parke, E. A., Mariuzza, R. A. & Kranz, D. M. (2000). Mapping the energy of superantigen Staphylococcus enterotoxin C3 recognition of an alpha/beta T cell receptor using alanine scanning mutagenesis. *J. Exp. Med.* **191**, 835–846.
48. Kjer-Nielsen, L., Clements, C. S., Purcell, A. W., Brooks, A. G., Whisstock, J. C., Burrows, S. R. *et al.* (2003). A structural basis for the selection of dominant alphabeta T cell receptors in antiviral immunity. *Immunity*, **18**, 53–64.

Edited by I. Wilson

(Received 2 October 2006; received in revised form 3 January 2007; accepted 6 January 2007)
Available online 12 January 2007